Casimir-Polder interaction between an atom and a periodic nanostructure

V. Yannopapas[1,2,*] and N. V. Vitanov[2,3]

[1]*Department of Materials Science, University of Patras, GR-26504 Patras, Greece*

[2]*Department of Physics, Sofia University, James Bourchier 5 blvd., BG-1164 Sofia, Bulgaria*

[3]*Institute of Solid State Physics, Bulgarian Academy of Sciences, Tsarigradsko chaussée 72, BG-1784 Sofia, Bulgaria*

(Received 26 October 2009; published 12 April 2010)

We present a theory for the calculation of the Casimir-Polder potential experienced by an atom near the surface of a nanostructure. The potential is found by means of the electrodynamic Green's tensor based on a layer-multiple-scattering method. We calculate the distance law of the Casimir-Polder potential for a monolayer of metallic and dielectric nanospheres arranged periodically on a square lattice. We find, in particular, that the Casimir-Polder potential for a metallic nanostructure is practically independent of the type of the metal from which the nanostructure is made. Also, the Casimir-Polder potential shows an exponential decay close to the nanostructure and an inverse power-law decrease away from it wherein the exponent depends on the size of the spheres of the nanostructure.

DOI: 10.1103/PhysRevA.81.042506 PACS number(s): 31.30.jh, 78.67.Bf, 42.50.Lc, 12.20.−m

I. INTRODUCTION

One of the most important manifestations of quantum fluctuations is the occurrence of van der Waals forces among atoms, molecules, and/or material bodies. Of particular interest is the potential experienced by an atom in the close vicinity of a surface: the exchange of virtual photons between the atom and the surface results in a net force on the atom. This type of interaction is known as Casimir-Polder (CP) potential and, originally, it was calculated by a standard normal-mode technique of quantum electrodynamics (QED) [1]. Recently, the presence the CP potential has been increasingly important in the context of atom chips and material traps where an atom is trapped by optical means [2–4]. When the atom trap is formed at a distance smaller than about a micron, the contribution of the CP interaction to the total trapping potential is comparable to that of the optical potential, even for large laser intensities.

Calculations of the CP potential are restricted to simple geometries such as planar surfaces [5–16], cylinders [17,18], and spheres [17,19–21]. However, theory and calculations for more complex geometries such as periodic arrays of scatterers or micro- and nanostructured surfaces is still lacking although there is an increasing interest in such structures which can provide a means to realize lattices of optical traps for individual particles, atoms, and Bose-Einstein condensates [3,4,22–25].

The advent of new computational techniques of classical electrodynamics in the context of photonic micro- and nanostructures has also enabled the development of new techniques which solve exactly Maxwell's equations with the exact boundary conditions. This way, they describe accurately the zero-point vacuum fluctuations and provide the van der Waals–Casimir forces for complex geometries via application of the fluctuation-dissipation theorem [26–29]. In this context, we present calculations for the CP potential of a neutral atom in close proximity to a two-dimensional (2D) lattice of nanospheres based on a fluctuational-electrodynamics approach [20,21]. The latter amounts to calculating the electromagnetic (EM) Green's tensor of the above lattice based on a layer-multiple-scattering method which is an efficient computational method for the study of the EM response of three-dimensional photonic structures consisting of nonoverlapping spheres [30–32] and axisymmetric nonspherical particles [33]. The layer-multiple-scattering method was originally introduced for the calculation of the transmission, reflection, and absorption coefficients of an EM wave incident on a composite slab consisting of a number of layers which can be either planes of nonoverlapping particles with the same 2D periodicity or homogeneous plates. For each plane of particles, the method calculates the full multipole expansion of the total multiply scattered wave field and deduces the corresponding transmission and reflection matrices in the plane-wave basis.

II. THEORY

Following the quantization scheme and perturbative approach of Ref. [20,21] we can find the CP potential experienced by an atom near a finite slab consisting of either several homogeneous slabs or planes of spheres with the same 2D periodicity or combinations of such. Namely

$$U_{CP}(\mathbf{r}) = 2\hbar\mu_0 \int_0^\infty d\xi \xi^2 \alpha(\mathrm{i}\xi) \sum_i G_{ii}^{EE}(\mathbf{r},\mathbf{r};\mathrm{i}\xi), \tag{1}$$

where α is the ground-state polarizability of a given atom and $G_{ii'}^{EE}$ the electric-field component of the EM Green's tensor associated with the trapping structure. For a finite slab of a metamaterial, the Green's tensor is given by

$$G_{ii'}^{EE}(\mathbf{r},\mathbf{r};\mathrm{i}\xi) = -\frac{i}{8\pi^2} \iint_{SBZ} d^2\mathbf{k}_\parallel \sum_{p\mathbf{g}} \frac{1}{c^2 K_{\mathbf{g};z}^+} v_{p\mathbf{g}\mathbf{k}_\parallel;i}(\mathbf{r}) \times \exp(-\mathrm{i}\mathbf{K}_\mathbf{g}^+ \cdot \mathbf{r}) e_{p;i'}(\mathbf{K}_\mathbf{g}^+) \tag{2}$$

with

$$v_{p\mathbf{g}\mathbf{k}_\parallel;i}(\mathbf{r}) = \sum_{p'\mathbf{g}'} R_{\mathbf{g}'p';\mathbf{g}p} \exp(-\mathrm{i}\mathbf{K}_{\mathbf{g}'}^- \cdot \mathbf{r}) e_{p';i}(\mathbf{K}_{\mathbf{g}'}^-) \tag{3}$$

$$\mathbf{K}_\mathbf{g}^\pm = (\mathbf{k}_\parallel + \mathbf{g},\ \pm[q^2 - (\mathbf{k}_\parallel + \mathbf{g})^2]^{1/2}) \tag{4}$$

and $q = \mathrm{i}\xi/c$. The vectors $\mathbf{g}$ denote the reciprocal-lattice vectors corresponding to the 2D periodic lattice of the plane of scatterers and $\mathbf{k}_\parallel$ is the reduced wave vector which lies within

*vyannop@upatras.gr

the surface Brillouin zone (SBZ) associated with the reciprocal lattice (see the appendix). The symbol $p = 1, 2$ refers to the two different polarizations states of the EM field. $\hat{\mathbf{e}}_1(\mathbf{K}_\mathbf{g}^\pm)$ and $\hat{\mathbf{e}}_2(\mathbf{K}_\mathbf{g}^\pm)$ are the polar and azimuthal unit vector normal to $\mathbf{K}_\mathbf{g}^\pm$, respectively. We note that the above expressions [Eqs. (2) and (3)] are derived from the transverse part of the general classical-wave Green's tensor [34].

$R_{\mathbf{g}'p';\mathbf{g}p}$ is the reflection matrix which provides the sum (over $\mathbf{g}$'s) of reflected beams generated by the incidence of plane wave from the left of the slab [30–32]. Details on how it is calculated can be found in the appendix. It contains the information for the multiple-scattering events which the vacuum fluctuations undergo within the plane of spheres. As such, its values depend on the angular-momentum cutoff $\ell_{\max}$. However, the distance $|\mathbf{r}|$ between the atom and the nanostructure appears in the CP potential only within the exponential functions (plane waves) of Eqs. (2) and (3). This is due to the fact that, away from the plane of spheres and in free space, the vacuum fluctuations are expressed in *plane* and not in *spherical* waves as it is the case for the fluctuations within the plane of spheres [30–32]. Therefore, the angular-momentum cutoff $\ell_{\max}$ needed for converged values of the CP potential is independent of the atom-plane distance and depends on (increases with) the lattice constant and the sphere size relative to the working wavelength. Moreover, since the main contribution to the CP potential stems from long wavelengths, the $\ell_{\max}$ convergence is rapid. The rate of convergence of the CP potential for the various atom-plane distances depends only on the number of the reciprocal-lattice vectors $\mathbf{g}$ in the plane-wave expansion of the vacuum fluctuations. However, due to the exponential decay of the plane waves in the imaginary frequency axis (see below) the number of the reciprocal-lattice vectors needed to achieve convergence is small.

The $\mathbf{k}_\parallel$-integration in Eq. (2) is performed within the area A_0 of the SBZ associated with a given 2D lattice. The spectral integration in Eq. (1) is done for imaginary frequencies $\omega = \mathrm{i}\xi$ provided that ϵ and μ contained therein are causal. In the calculations that follow, the SBZ integration of Eq. (1) is performed by subdividing progressively the SBZ into smaller and smaller squares, within which a nine-point integration formula [35] is very efficient. Using this formula we achieved excellent convergence with a total of 576 points in the SBZ. Also, the inclusion of 13 reciprocal-lattice $\mathbf{g}$ vectors in the summation of Eq. (2) provided converged results for all distances. In the spherical-wave expansion of the field within the plane of spheres we have considered terms up to an angular-momentum cutoff $\ell_{\max} = 3$. Finally, since the frequency integration is performed along the imaginary axis, the lattice sum over the reciprocal-lattice vectors $\mathbf{g}$ in Eq. (2) is performed by summation in direct space since Ewald-summation schemes do not converge [31]. We note that the method of Refs. [30–32] calculates accurately the transmission, reflection, and absorption coefficients from slabs of spheres. It incorporates both propagating (far-field) and evanescent (near-field) EM waves. In this respect, the method presented here can, in principle, calculate both retarded and nonretarded limits of the Casimir-Polder interaction. However, for the atom-nanostructure separations considered here, the nonretarded contribution dominates the retarded one.

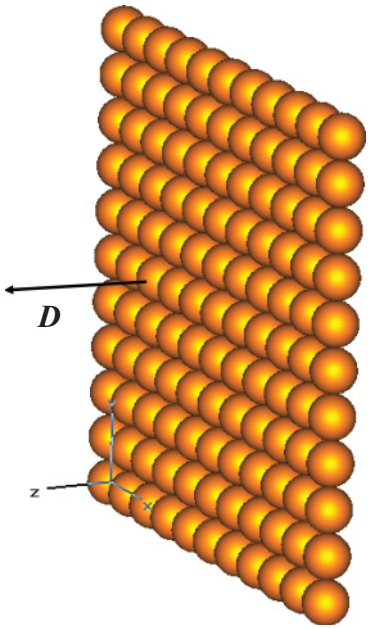

FIG. 1. (Color online) Monolayer of spherical nanoparticles. D is the distance of atom from the surface of a nanoparticle.

III. RESULTS

The above formalism is first applied to the case of a 2D square lattice (monolayer) of period $a = 50$ nm, whose lattice sites are occupied by spherical nanoparticles of radius $S = 25$ nm, i.e., we deal with a 2D array of close-packed spheres (see Fig. 1). We study spheres made from metal (gold, silver, copper) and dielectric (polystyrene). The dielectric functions $\epsilon(\mathrm{i}\xi)$ of the above materials needed for the calculation of the Green's tensor of Eq. (2) are obtained according to the formula [36]

$$\epsilon(\mathrm{i}\xi) = 1 + \sum_{j=1}^{5} \frac{f_j}{\omega_j^2 + g_j\xi + \xi^2}, \tag{5}$$

where the fitting coefficients $\omega_j, f_j, g_j, j = 1, \ldots, 5$ for each of the above materials are taken from available experimental data [36]. We note that as dielectric material we have restricted the simulations to polystyrene due to the lack of tabulated data $(\omega_j, f_j, g_j,\ j = 1, \ldots, 5)$ for dielectrics usually used in the fabrication of nanostructures. Near the nanostructures described above we place a Cs atom whose polarizability tensor $\alpha(\mathrm{i}\xi)$ needed in Eq. (1) is taken from first-principles atomic-structure calculations [37]. We note that the above polarizability refers to an atom being in the ground state. If the atom is in an excited state, there exists an additional resonant term in the total CP potential which is proportional to the real part of the EM Green's tensor calculated at the frequency difference between the ground and excited states [38]. This case, however, will not be considered here since the contribution of the excited states is important only when the atomic element is chosen such that the frequency difference between the ground and an excited states matches the frequency of a material resonance of the nanostructure [38], e.g., with a surface plasmon resonance or a negative refractive-index resonance.

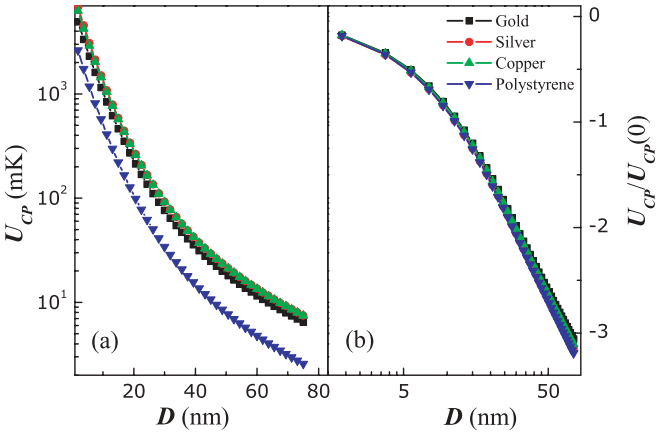

FIG. 2. (Color online) The CP potential experienced by a Cs atom as a function of distance D from a 2D square lattice (lattice constant $a = 50$ nm) of 25-nm nanospheres made from gold, silver, copper, and polystyrene in (a) log-linear and (b) log-log scale. The CP potential is calculated along a direction normal to the plane of spheres and passing through the center of one of the spheres. Note that in (b) we actually plot $\log_{10}[U_{CP}(D)/U_{CP}(D_0)]$, where $D_0 = 25.6$ nm is the distance from the sphere center.

Figure 2 shows the CP potential felt by a Cs atom placed in the proximity of a 2D square lattice of metal (gold, silver, copper) and dielectric (polystyrene) nanospheres. The CP potential is calculated along a direction normal to the lattice of spheres and passing through the center of one of the spheres, for various distances D from the surface of that sphere. First, we note that the value of the CP potential when the Cs atom is placed (almost) on top of a sphere is shown only for completeness since for atomic distances from the surface of a nanosphere, the macroscopic description of the nanospheres is no longer valid since there occur several other effects such as Born-repulsive potentials stemming from exchange and electrostatic interactions which can be accounted for only through a microscopic description of a nanosphere [39,40]. From Fig. 2(a) it is evident that the CP potential is practically the same for all arrays of metallic spheres while it is significantly weaker for the case of polystyrene spheres due to the smaller values of $\epsilon(i\xi)$ at low frequencies [36]. Especially, the curves for copper and silver are almost indistinguishable. These observations suggest that the main contribution to the CP potential stems from the long-wavelength vacuum fluctuations where the metals are essentially perfect conductors and the actual (large) values assumed by the dielectric function are not important. It is also worth noting that, from Fig. 2(b) where we plot the logarithm of dimensionless CP potential, it is clear that the CP potential for distances $D > 20$ nm obeys the same power law (average exponent $\nu = 2.67 \pm 0.03$) regardless of the type of material. For $D < 20$ nm, the CP potential shows a linear behavior in the log-linear scale, suggesting, practically, an exponential decay or power-law decay with large exponent when the atom is close to the surface of the nanostructure. A similar spatial dependence, i.e., a very fast decay close to the surface and slower power-law decrease away from it, has been reported for the van der Waals–Casimir force between two metallic nanospheres [26] as well as between a nanoparticle and a planar surface [41,42].

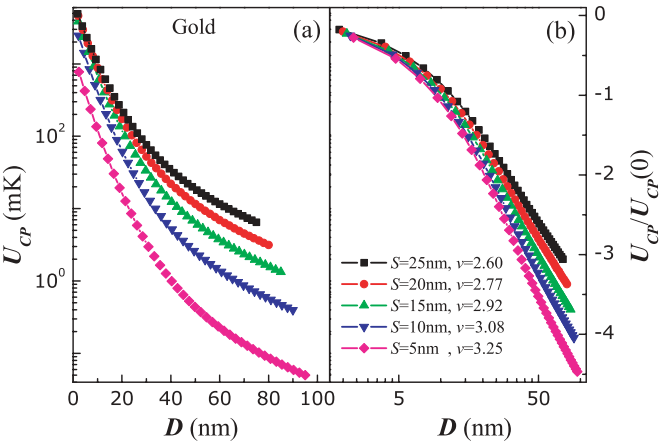

FIG. 3. (Color online) The CP potential experienced by a Cs atom as a function of distance D from a 2D square lattice (lattice constant $a = 50$ nm) of gold nanospheres for various radii, i.e., $S = 25$, 20, 15, 10, and 5 nm in (a) log-linear and (b) log-log scale.

Since the CP potential for the metallic nanostructures does not depend dramatically on the type of the material from which the nanostructure is made, we focus on a 2D lattice of gold nanospheres. In Fig. 3 we calculate the CP potential for gold nanostructures with the same period ($a = 50$ nm) but different sphere sizes (shown in the legend). As expected, as the sphere size decreases, the nanostructure becomes more dilute, and, naturally, the amount of vacuum fluctuations is reduced resulting in a suppressed CP potential experienced by the atom. We note, however, that from Fig. 3(b) it is clear that the long-distance power law is not the same for the various sphere sizes. For the case of 25 nm spheres the exponent is $\nu = 2.60$ while for 5-nm spheres it is $\nu = 3.25$. All the inverse power-law exponents ν for the various sphere sizes are shown in the legend of Fig. 3 (the same applies to Fig. 4). Since we keep the lattice constant fixed ($a = 50$ nm), the exponent ν essentially depends on the surface coverage of the spheres, i.e., it decreases with increasing surface coverage. Dependence of the inverse power-law exponent on the surface coverage has also been predicted for the case of the Casimir energy between a flat and a corrugated surface [43]. Namely

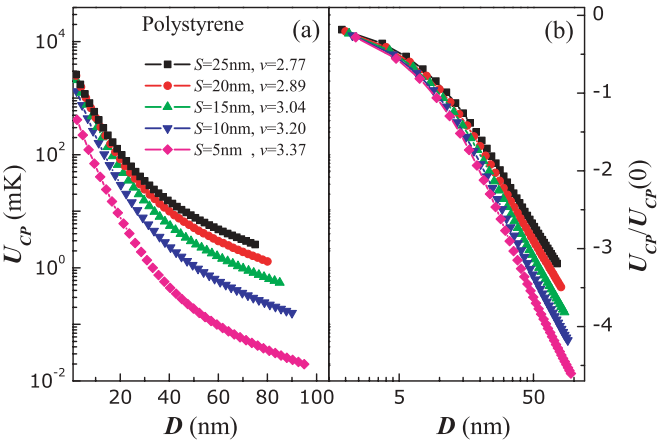

FIG. 4. (Color online) The same as Fig. 3 but for a 2D square lattice of polystyrene spheres.

a noninteger overall exponent for the inverse power law has been reported due to the contribution of terms corresponding to exponents higher than 3. The contribution of each component is proportional to a power of the ratio of the groove height to the period of the corrugated surface [43]; the latter ratio is similar to the ratio of the sphere radius to the 2D lattice constant.

According to Fig. 3, the differences in the rate of decay of the CP potential for the different sphere radii increase with the distance of the atom from the plane of spheres. It is well known [36] that, at short distances, the CP potential (and generally the Casimir–van der Waals interactions) is determined by the low-frequency components of the reflection matrix, while, for larger distances higher-frequency components become more significant in Eq. (1). The latter contribution is much more important as the density of spheres increases (and subsequently the density of EM modes) providing additional components to the CP potential and delaying, this way, its decay with distance.

Figure 4 is the same as Fig. 3 but for a 2D square lattice of polystyrene nanospheres. We observe a quite similar behavior with that of the gold nanostructures of Fig. 3, implying that the CP potential is described by same distance laws which are more or less material independent.

A general remark which applies to Figs. 2–4 is the fact that the CP potential assumes very large values (of the order of several kelvins) even for distances of about 50 nm away from the nanostructure. This is a serious drawback when one attempts to trap cold atoms in lattices near illuminated nanostructures via near-field optical potentials: great laser powers are needed so that the optical potential could cancel the CP potential and create a potential minimum within which cold atoms can be trapped. Of course, far away from the nanostructure, the CP potential is small; however, the optical potential landscape is a near-field effect which decays in space with, more or less, the same rate with CP potential. This means that, although the optical potential would cancel the CP potential for long distances with moderate laser power, the total (optical + CP) potential would be too shallow to prevent trapped atoms from escaping to free space.

Nanostructures such as those studied here have already been realized in the laboratory [44,45]. Of course, the arrays of nanoparticles are grown on top of planar substrates which sometimes affect the optical response of the nanostructures, e.g., its reflection and transmittance spectra [46]. We have repeated our calculations by the inclusion of a dielectric (quartz) substrate supporting the array of nanospheres without, however, any effect on the presented graphs. This is an anticipated result since the Casimir-Polder interaction is a purely surface phenomenon.

IV. CONCLUSION

In conclusion, we have presented a formalism for the calculation of the CP potential experienced by an atom residing near a periodic nanostructure. The method is based on a rigorous multiple-scattering technique for the calculation of the Green's tensor of the EM field. Using the above formalism, we have shown that the CP potential is practically independent of the material from which the nanostructure is made. Also, for short distances from the nanostructure, the CP potential decays exponentially while for longer distances it exhibits a power-law decrease. The exponent of the power law increases as the nanostructure becomes more dilute.

ACKNOWLEDGMENTS

This work has been supported by the European Commission's projects EMALI and FASTQUAST and the Bulgarian NSF Grant Nos. VU-F-205/06, VU-I-301/07, and D002-90/08.

APPENDIX

A plane EM wave of angular frequency ω and wave vector $\mathbf{q}$, propagating in a homogeneous medium characterized by a dielectric function $\epsilon(\omega)\epsilon_0$ and a magnetic permeability $\mu(\omega)\mu_0$, where ϵ_0, μ_0 are the dielectric constant and the magnetic permeability of vacuum, has an electric-field component

$$\mathbf{E}(\mathbf{r},t) = \mathrm{Re}[\mathbf{E}(\mathbf{r})\exp(-\mathrm{i}\omega t)] \tag{A1}$$

defined by

$$\mathbf{E}(\mathbf{r}) = \mathbf{E}_0(\mathbf{q})\exp(\mathrm{i}\mathbf{q}\cdot\mathbf{r}). \tag{A2}$$

The magnitude of the wave vector is given by $q = \sqrt{\mu\epsilon}\,\omega/c$, where $c = 1/\sqrt{\mu_0\epsilon_0}$ is the velocity of light in vacuum. $\mathbf{E}_0(\mathbf{q}) \equiv E_0(\mathbf{q})\hat{\mathbf{p}}$, where E_0 denotes the magnitude and $\hat{\mathbf{p}}$, a unit vector, the polarization of the electric field. We need not write down explicitly the magnetic-field component of the wave. The plane wave given by Eq. (A2) is expanded in spherical waves as follows [31,32]

$$\mathbf{E}(\mathbf{r}) = \sum_{\ell=1}^{\infty}\sum_{m=-\ell}^{\ell}\left(\frac{\mathrm{i}}{q}\mathrm{a}_{\ell m}^{0E}\nabla\times j_\ell(qr)\mathbf{X}_{\ell m}(\hat{\mathbf{r}}) + \mathrm{a}_{\ell m}^{0H} j_\ell(qr)\mathbf{X}_{\ell m}(\hat{\mathbf{r}})\right), \tag{A3}$$

where the coefficients $\mathrm{a}_{\ell m}^{0P}$, $P = E, H$, are constants to be determined and $j_\ell(qr)$ is a spherical Bessel function. For $\ell \geqslant 1$, the vector spherical harmonics $\mathbf{X}_{\ell m}(\hat{\mathbf{r}})$, $\hat{\mathbf{r}} = (\theta,\ \phi)$, are given, in spherical coordinates, by

$$\begin{aligned}\sqrt{\ell(\ell+1)}\mathbf{X}_{\ell m}(\hat{\mathbf{r}}) = {}& \left[\alpha_\ell^{-m}\cos\theta e^{\mathrm{i}\phi}Y_\ell^{m-1}(\hat{\mathbf{r}}) - m\sin\theta Y_\ell^m(\hat{\mathbf{r}}) + \alpha_\ell^m\cos\theta e^{-\mathrm{i}\phi}Y_\ell^{m+1}(\hat{\mathbf{r}})\right]\hat{\mathbf{e}}_1 \\ & + \mathrm{i}\left[\alpha_\ell^{-m}e^{\mathrm{i}\phi}Y_\ell^{m-1}(\hat{\mathbf{r}}) - \alpha_\ell^m e^{-\mathrm{i}\phi}Y_\ell^{m+1}(\hat{\mathbf{r}})\right]\hat{\mathbf{e}}_2,\end{aligned} \tag{A4}$$

where Y_ℓ^m denotes a spherical harmonic as usual, $\hat{\mathbf{e}}_1$, $\hat{\mathbf{e}}_2$ are the polar and azimuthal unit vectors, respectively, and

$$\alpha_\ell^m \equiv \tfrac{1}{2}[(\ell-m)(\ell+m+1)]^{1/2}. \tag{A5}$$

By definition $\mathbf{X}_{00}(\hat{\mathbf{r}}) = 0$.

We now consider a sphere of radius S with its center at the origin of coordinates and assume that its relative dielectric function and/or magnetic permeability, in general complex functions of ω, are different from those of the surrounding medium. When the plane wave described by Eq. (A3) is incident on the sphere, it is scattered by it, so that the wavefield outside the sphere consists of the incident wave (A3) and a corresponding scattered wave, which can be expanded in

spherical waves as follows

$$\mathbf{E}_{\rm sc}(\mathbf{r}) = \sum_{\ell=1}^{\infty}\sum_{m=-\ell}^{\ell}\left(\frac{\mathrm{i}}{q}\mathrm{a}_{\ell m}^{+E}\nabla\times h_\ell^+(qr)\mathbf{X}_{\ell m}(\hat{\mathbf{r}}) + \mathrm{a}_{\ell m}^{+H}h_\ell^+(qr)\mathbf{X}_{\ell m}(\hat{\mathbf{r}})\right), \tag{A6}$$

where $h_\ell^+(qr)$ is the spherical Hankel function. Because of the spherical symmetry of the scatterer, each spherical wave in Eq. (A3) scatters independently of all others; therefore

$$\mathrm{a}_{\ell m}^{+P} = T_\ell^P \mathrm{a}_{\ell m}^{0P}. \tag{A7}$$

Explicit expressions for T_ℓ^E, T_ℓ^H are given in Refs. [31,32]. Provided qS is not much larger than unity, a limited number of partial waves, corresponding to $\ell \leqslant \ell_{\max}$, is sufficient for the description of the scattered field. We note, however, that when multiple scattering from a plane of spheres is considered, $\ell_{\max}$ must be determined from the requirement of convergence as far as the scattering by the plane is concerned, and in this respect $\ell_{\max}$ may be greater than that obtained for scattering by a single sphere.

We consider a plane of spheres at $z=0$ in which case the spheres, which do not overlap with each other, are centered on the sites $\mathbf{R}_n$ of a given 2D lattice. We define the 2D reciprocal vectors $\mathbf{g}$, and the SBZ corresponding to this lattice in the usual manner [31,32].

Let the plane wave, described by Eq. (A2), be incident on this plane of spheres. We can always write the component of its wave vector parallel to the plane of spheres, as follows

$$\mathbf{q}_\parallel = \mathbf{k}_\parallel + \mathbf{g}', \tag{A8}$$

where the reduced wave vector $\mathbf{k}_\parallel$ lies in the SBZ and $\mathbf{g}'$ is a certain reciprocal vector. In what follows we shall write the wave vector of a plane wave of given $q=\sqrt{\mu\epsilon}\,\omega/c$ and given $\mathbf{q}_\parallel = \mathbf{k}_\parallel + \mathbf{g}$ as follows

$$\mathbf{K}_{\mathbf{g}}^{\pm} = \{\mathbf{k}_\parallel + \mathbf{g},\ \pm[q^2 - (\mathbf{k}_\parallel + \mathbf{g})^2]^{1/2}\}, \tag{A9}$$

where the $+,-$ sign defines the sign of the z component of the wave vector.

We write the electric field of the incident wave in the form

$$\mathbf{E}_{\rm in}^{s'}(\mathbf{r}) = \sum_{i'=1}^{2}[E_{\rm in}]_{\mathbf{g}'i'}^{s'}\exp\left(\mathrm{i}\mathbf{K}_{\mathbf{g}'}^{s'}\cdot\mathbf{r}\right)\hat{\mathbf{e}}_{i'}, \tag{A10}$$

where $s'=+(-)$ corresponds to a propagating or decaying wave incident on the plane of spheres from the left (right) and $\hat{\mathbf{e}}_1$, $\hat{\mathbf{e}}_2$ are the polar and azimuthal unit vectors, respectively, which are perpendicular to $\mathbf{K}_{\mathbf{g}'}^{s'}$. In the same manner [according to Eq. (A9)] we define, for given $\mathbf{k}_\parallel$ and q, a wave vector $\mathbf{K}_{\mathbf{g}}^{s}$ and the corresponding $\hat{\mathbf{e}}_i$ for any $\mathbf{g}$ and $s=\pm$. In this way we can expand the electric-field component of an EM wave into p- and s-polarized transverse plane waves, i.e., polarized along $\hat{\mathbf{e}}_1$ and $\hat{\mathbf{e}}_2$, respectively. We note that, in the case of a decaying wave, the unit vectors $\hat{\mathbf{e}}_1$ and $\hat{\mathbf{e}}_2$ are complex but they are still orthonormal ($\hat{\mathbf{e}}_i\cdot\hat{\mathbf{e}}_j=\delta_{ij}$, $i,j=1,2$). The coefficients $\mathrm{a}_{\ell m}^{0P}$ in the expansion (A3) of the plane wave (A10) can be written in the following form

$$\mathrm{a}_{\ell m}^{0P} = \sum_{i'=1}^{2}A_{\ell m;i'}^{0P}\left(\mathbf{K}_{\mathbf{g}'}^{s'}\right)[E_{\rm in}]_{\mathbf{g}'i'}^{s'}, \quad \text{for} \quad P=E,H, \tag{A11}$$

where

$$\begin{aligned}\mathbf{A}_{\ell m}^{0E}\left(\hat{\mathbf{K}}_{\mathbf{g}'}^{s'}\right) = \frac{4\pi\mathrm{i}^\ell(-1)^{m+1}}{\sqrt{\ell(\ell+1)}}\Big\{&\mathrm{i}\Big[\alpha_\ell^m e^{\mathrm{i}\phi}Y_\ell^{-m-1}\left(\hat{\mathbf{K}}_{\mathbf{g}'}^{s'}\right)\\ &-\alpha_\ell^{-m}e^{-\mathrm{i}\phi}Y_\ell^{-m+1}\left(\hat{\mathbf{K}}_{\mathbf{g}'}^{s'}\right)\Big]\hat{\mathbf{e}}_1\\ &-\Big[\alpha_\ell^m\cos\theta e^{\mathrm{i}\phi}Y_\ell^{-m-1}\left(\hat{\mathbf{K}}_{\mathbf{g}'}^{s'}\right)+m\sin\theta Y_\ell^{-m}\left(\hat{\mathbf{K}}_{\mathbf{g}'}^{s'}\right)\\ &+\alpha_\ell^{-m}\cos\theta e^{-\mathrm{i}\phi}Y_\ell^{-m+1}\left(\hat{\mathbf{K}}_{\mathbf{g}'}^{s'}\right)\Big]\hat{\mathbf{e}}_2\Big\}\end{aligned} \tag{A12}$$

and

$$\begin{aligned}\mathbf{A}_{\ell m}^{0H}\left(\hat{\mathbf{K}}_{\mathbf{g}'}^{s'}\right) = \frac{4\pi\mathrm{i}^\ell(-1)^{m+1}}{\sqrt{\ell(\ell+1)}}\Big\{&\Big[\alpha_\ell^m\cos\theta e^{\mathrm{i}\phi}Y_\ell^{-m-1}\left(\hat{\mathbf{K}}_{\mathbf{g}'}^{s'}\right)\\ &+m\sin\theta Y_\ell^{-m}\left(\hat{\mathbf{K}}_{\mathbf{g}'}^{s'}\right)+\alpha_\ell^{-m}\cos\theta e^{-\mathrm{i}\phi}\\ &\times Y_\ell^{-m+1}\left(\hat{\mathbf{K}}_{\mathbf{g}'}^{s'}\right)\Big]\hat{\mathbf{e}}_1+\mathrm{i}\Big[\alpha_\ell^m e^{\mathrm{i}\phi}Y_\ell^{-m-1}\left(\hat{\mathbf{K}}_{\mathbf{g}'}^{s'}\right)\\ &-\alpha_\ell^{-m}e^{-\mathrm{i}\phi}Y_\ell^{-m+1}\left(\hat{\mathbf{K}}_{\mathbf{g}'}^{s'}\right)\Big]\hat{\mathbf{e}}_2\Big\},\end{aligned} \tag{A13}$$

where θ, ϕ are the angular variables ($\hat{\mathbf{K}}_{\mathbf{g}'}^{s'}$) of $\mathbf{K}_{\mathbf{g}'}^{s'}$.

Because of the 2D periodicity of the plane of spheres, the wave scattered from it, when the wave (A10) is incident on it, has the following form

$$\begin{aligned}&\mathbf{E}_{\rm sc}(\mathbf{r})\\ &=\sum_{\ell=1}^{\ell_{\max}}\sum_{m=-\ell}^{\ell}\left(\frac{\mathrm{i}}{q}\mathrm{b}_{\ell m}^{+E}\nabla\times\sum_{\mathbf{R}_n}\exp(\mathrm{i}\mathbf{k}_\parallel\cdot\mathbf{R}_n)h_\ell^+(qr_n)\mathbf{X}_{\ell m}(\hat{\mathbf{r}}_n)\right.\\ &\left.+\mathrm{b}_{\ell m}^{+H}\sum_{\mathbf{R}_n}\exp(\mathrm{i}\mathbf{k}_\parallel\cdot\mathbf{R}_n)h_\ell^+(qr_n)\mathbf{X}_{\ell m}(\hat{\mathbf{r}}_n)\right),\end{aligned} \tag{A14}$$

where $\mathbf{r}_n=\mathbf{r}-\mathbf{R}_n$. The coefficients $\mathrm{b}_{\ell m}^{+P}$, which depend linearly on the amplitude of the incident wave, can be written as follows

$$\mathrm{b}_{\ell m}^{+P} = \sum_{i'=1}^{2}B_{\ell m;i'}^{+P}\left(\mathbf{K}_{\mathbf{g}'}^{s'}\right)[E_{\rm in}]_{\mathbf{g}'i'}^{s'}. \tag{A15}$$

We obtain $\mathbf{B}_{\ell m}^{+P}$ in terms of the coefficients $\mathbf{A}_{\ell m}^{0P}$ which are given by Eqs. (A12) and (A13), by solving the following system of linear equations [31,32]

$$\begin{aligned}&\sum_{P'=E,H}\sum_{\ell'=1}^{\ell_{\max}}\sum_{m'=-\ell'}^{\ell'}\left[\delta_{PP'}\delta_{\ell\ell'}\delta_{mm'}-T_\ell^P\Omega_{\ell m;\ell' m'}^{PP'}\right]B_{\ell' m';i'}^{+P'}\left(\mathbf{K}_{\mathbf{g}'}^{s'}\right)\\ &\quad=T_\ell^P\mathrm{A}_{\ell m;i'}^{0P}\left(\mathbf{K}_{\mathbf{g}'}^{s'}\right)\end{aligned} \tag{A16}$$

The matrix elements $\Omega_{\ell m;\ell' m'}^{PP'}$ depend on the geometry of the plane, on the reduced wave vector $\mathbf{k}_\parallel$, and on the frequency ω of the incident wave; they depend also on the dielectric function of the medium surrounding the spheres, but they do not depend on the scattering properties of the individual spheres. Explicit expressions for these matrix elements are given in Refs. [31,32].

Finally, the scattered wave (A14) is expressed as a sum of plane waves as follows

$$\mathbf{E}_{\rm sc}^{s}(\mathbf{r}) = \sum_{i=1}^{2}\sum_{\mathbf{g}}[E_{\rm sc}]_{\mathbf{g}i}^{s}\exp\left(\mathrm{i}\mathbf{K}_{\mathbf{g}}^{s}\cdot\mathbf{r}\right)\hat{\mathbf{e}}_i, \tag{A17}$$

where the superscript $s = +(-)$ holds for $z > 0$ ($z < 0$). The scattered wave consists, in general, of a number of diffracted beams corresponding to different $\mathbf{g}$ vectors. The coefficients in Eq. (A17) are given by

$$[E_{\rm sc}]^s_{\mathbf{g}i} = \sum_{P=E,H} \sum_{\ell=1}^{\ell_{\max}} \sum_{m=-\ell}^{\ell} \Delta^P_{\ell m;i}(\mathbf{K}^s_{\mathbf{g}}) B^{+P}_{\ell m;i'}(\mathbf{K}^{s'}_{\mathbf{g}'}), \tag{A18}$$

where

$$\Delta^E_{\ell m}(\mathbf{K}^s_{\mathbf{g}}) = \frac{2\pi(-\mathrm{i})^\ell}{qA_0K^+_{\mathbf{g}z}\sqrt{\ell(\ell+1)}}\{\mathrm{i}[\alpha^{-m}_\ell e^{\mathrm{i}\phi}Y^{m-1}_\ell(\hat{\mathbf{K}}^s_{\mathbf{g}}) - \alpha^m_\ell e^{-\mathrm{i}\phi}Y^{m+1}_\ell(\hat{\mathbf{K}}^s_{\mathbf{g}})]\hat{\mathbf{e}}_1 - [\alpha^{-m}_\ell \cos\theta e^{\mathrm{i}\phi}Y^{m-1}_\ell(\hat{\mathbf{K}}^s_{\mathbf{g}}) - m\sin\theta Y^m_\ell(\hat{\mathbf{K}}^s_{\mathbf{g}}) + \alpha^m_\ell \cos\theta e^{-\mathrm{i}\phi}Y^{m+1}_\ell(\hat{\mathbf{K}}^s_{\mathbf{g}})]\hat{\mathbf{e}}_2\} \tag{A19}$$

$$\Delta^H_{\ell m}(\mathbf{K}^s_{\mathbf{g}}) = \frac{2\pi(-\mathrm{i})^\ell}{qA_0K^+_{\mathbf{g}z}\sqrt{\ell(\ell+1)}}\{[\alpha^{-m}_\ell \cos\theta e^{\mathrm{i}\phi}Y^{m-1}_\ell(\hat{\mathbf{K}}^s_{\mathbf{g}}) - m\sin\theta Y^m_\ell(\hat{\mathbf{K}}^s_{\mathbf{g}}) + \alpha^m_\ell \cos\theta e^{-\mathrm{i}\phi}Y^{m+1}_\ell(\hat{\mathbf{K}}^s_{\mathbf{g}})]\hat{\mathbf{e}}_1 + \mathrm{i}[\alpha^{-m}_\ell e^{\mathrm{i}\phi}Y^{m-1}_\ell(\hat{\mathbf{K}}^s_{\mathbf{g}}) - \alpha^m_\ell e^{-\mathrm{i}\phi}Y^{m+1}_\ell(\hat{\mathbf{K}}^s_{\mathbf{g}})]\hat{\mathbf{e}}_2\}, \tag{A20}$$

where θ, ϕ denote the angular variables $(\hat{\mathbf{K}}^s_{\mathbf{g}})$ of $\mathbf{K}^s_{\mathbf{g}}$. We point out that, according to Eq. (A18), $[E_{sc}]^s_{\mathbf{g}i}$ depend on the incident plane wave through the coefficients $B^{+P}_{\ell m;i'}(\mathbf{K}^{s'}_{\mathbf{g}'})$. These coefficients are to be evaluated for an incident plane wave with parallel wave vector $\mathbf{k}_\parallel + \mathbf{g}'$, incident from the left (right) corresponding to $s' = +(-)$, with an electric field, along the i'th direction, of magnitude equal to unity. In other words, $B^{+P}_{\ell m;i'}(\mathbf{K}^{s'}_{\mathbf{g}'})$ are calculated from Eq. (A16), substituting, on the right-hand side of this equation, $A^{0P}_{\ell m;i'}(\mathbf{K}^{s'}_{\mathbf{g}'})$ from Eqs. (A12) and (A13).

When a plane wave (A10) is incident on the plane of spheres from the left, the reflected wave on the left of the plane of spheres is given by

$$\mathbf{E}^-_{rf}(\mathbf{r}) = \sum_{i=1}^{2}\sum_{\mathbf{g}}[E_{rf}]^-_{\mathbf{g}i}\exp(\mathrm{i}\mathbf{K}^-_{\mathbf{g}}\cdot\mathbf{r})\hat{\mathbf{e}}_i \quad z<0 \tag{A21}$$

with

$$[E_{rf}]^-_{\mathbf{g}i} = [E_{\rm sc}]^-_{\mathbf{g}i} = \sum_{i'} R_{\mathbf{g}i;\mathbf{g}'i'}[E_{\rm in}]^+_{\mathbf{g}'i'}. \tag{A22}$$

Using Eq. (A18) we finally obtain

$$R_{\mathbf{g}i;\mathbf{g}'i'} = \sum_{P=E,H}\sum_{\ell=1}^{\ell_{\max}}\sum_{m=-\ell}^{\ell}\Delta^P_{\ell m;i}(\mathbf{K}^s_{\mathbf{g}})B^{+P}_{\ell m;i'}(\mathbf{K}^{s'}_{\mathbf{g}'}). \tag{A23}$$

[1] H. B. G. Casimir and D. Polder, Phys. Rev. **73**, 360 (1948).

[2] M. J. Renn, D. Montgomery, O. Vdovin, D. Z. Anderson, C. E. Wieman, and E. A. Cornell, Phys. Rev. Lett. **75**, 3253 (1995); H. Ito, T. Nakata, K. Sakaki, M. Ohtsu, K. I. Lee, and W. Jhe, *ibid.* **76**, 4500 (1996); J. Yin *et al.*, J. Opt. Soc. Am. B **15**, 25 (1998); A. H. Barnett, S. P. Smith, M. Olshanii, K. S. Johnson, A. W. Adams, and M. Prentiss, Phys. Rev. A **61**, 023608 (2000); J. Arlt, K. Dholakia, J. Soneson, and E. M. Wright, *ibid.* **63**, 063602 (2001); J. P. Burke, S. T. Chu, G. W. Bryant, C. J. Williams, and P. S. Julienne, *ibid.* **65**, 043411 (2002); V. I. Balykin, K. Hakuta, F. L. Kien, J. Q. Liang, and M. Morinaga, *ibid.* **70**, 011401(R) (2004); F. Le Kien, V. I. Balykin, and K. Hakuta, *ibid.* **70**, 063403 (2004); X. Luo *et al.*, Opt. Lett. **29**, 2145 (2004); D. Rychtarik, B. Engeser, H. C. Nagerl, and R. Grimm, Phys. Rev. Lett. **92**, 173003 (2004); E. Moreno, A. I. Fernandez-Dominguez, J. Ignacio Cirac, F. J. Garcia-Vidal, and L. Martin-Moreno, *ibid.* **95**, 170406 (2005).

[3] J. Bravo-Abad, M. Ibanescu, J. D. Joannopoulos, and M. Soljačić, Phys. Rev. A **74**, 053619 (2006).

[4] V. Yannopapas and N. V. Vitanov, Phys. Stat. Sol. (RRL), **2**, 287 (2008); J. Phys.: Condens. Matter **21**, 245901 (2009).

[5] M. J. Renne, Physica A **53**, 193 (1971); **56**, 125 (1971).

[6] P. W. Milonni and M. L. Shih, Phys. Rev. A **45**, 4241 (1992).

[7] F. Zhou and L. Spruch, Phys. Rev. A **52**, 297 (1995).

[8] M. M. Boström and B. E. Sernelius, Phys. Rev. A **61**, 052703 (2000).

[9] A. D. McLachlan, Proc. R. Soc. A **271**, 387 (1963); Mol. Phys. **7**, 381 (1963).

[10] G. S. Agarwal, Phys. Rev. A **11**, 243 (1975).

[11] J. M. Wylie and J. E. Sipe, Phys. Rev. A **30**, 1185 (1984).

[12] C. Girard, J. Chem. Phys. **85**, 6750 (1986).

[13] C. Girard and C. Girardet, J. Chem. Phys. **86**, 6531 (1987).

[14] R. Vasile, R. Messina, and R. Passante, Phys. Rev. A **79**, 062106 (2009).

[15] B. S. Skagerstam, P. K. Rekdal, and A. H. Vaskinn, Phys. Rev. A **80**, 022902 (2009).

[16] A. M. Contreras Reyes and C. Eberlein, Phys. Rev. A **80**, 032901 (2009).

[17] A. M. Marvin and F. Toigo, Phys. Rev. A **25**, 782 (1982).

[18] M. Boustimi, J. Baudon, P. Candori, and J. Robert, Phys. Rev. B **65**, 155402 (2002).

[19] C. Girard, S. Maghezzi, and F. Hache, J. Chem. Phys. **91**, 5509 (1989).

[20] S. Y. Buhmann, H. T. Dung, and D.-G. Welsch, J. Opt. B-Quantum S. O. **6**, S127 (2004).

[21] A. Sambale, S. Y. Buhmann, and S. Scheel, Phys. Rev. A **81**, 012509 (2010).

[22] M. I. Antonoyiannakis and J. B. Pendry, Europhys. Lett. **40**, 613 (1997).

[23] Z. Lu *et al.*, Opt. Express **14**, 2228 (2006).

[24] A. Rahmani and P. C. Chaumet, Opt. Express **14**, 6353 (2006).

[25] V. Yannopapas, Phys. Rev. B **78**, 045412 (2008).

[26] V. Yannopapas and N. V. Vitanov, Phys. Rev. Lett. **99**, 120406 (2007).

[27] V. Yannopapas, Phys. Rev. B **76**, 235415 (2007).

[28] A. Rodriguez, M. Ibanescu, D. Iannuzzi, F. Capasso, J. D. Joannopoulos, and S. G. Johnson, Phys. Rev. Lett. **99**, 080401 (2007).

[29] A. Rodriguez, M. Ibanescu, D. Iannuzzi, J. D. Joannopoulos, and S. G. Johnson, Phys. Rev. A **76**, 032106 (2007).

[30] N. Stefanou, V. Karathanos, and A. Modinos, J. Phys.: Condens. Matter **4**, 7389 (1992).
[31] N. Stefanou, V. Yannopapas, and A. Modinos, Comput. Phys. Commun. **113**, 49 (1998).
[32] N. Stefanou, V. Yannopapas, and A. Modinos, Comput. Phys. Commun. **132**, 189 (2000).
[33] G. Gantzounis and N. Stefanou, Phys. Rev. B **73**, 035115 (2006).
[34] R. Sainidou, N. Stefanou, and A. Modinos, Phys. Rev. B **69**, 064301 (2004).
[35] M. Abramowitz and I. A. Stegun, *Handbook of Mathematical Functions* (Dover, New York, 1965).
[36] V. A. Parsegian, *Van der Waals Forces* (Cambridge University Press, Cambridge, UK, 2006).
[37] A. Derevianko and S. G. Porsev, Phys. Rev. A **65**, 053403 (2002).
[38] A. Sambale, D.-G. Welsch, H. T. Dung, and S. Y. Buhmann, Phys. Rev. A **78**, 053828 (2008).
[39] J. X. Lu and W. H. Marlow, Phys. Rev. A **52**, 2141 (1995); J. X. Lu, W. H. Marlow, and V. Aunachalam, J. Colloid Interface Sci. **181**, 429 (1996).
[40] I. Baraille, M. Rérat, and P. Mora, Phys. Rev. B **73**, 075410 (2006).
[41] C. Noguez, C. E. Román-Velázquez, R. Esquivel-Sirvent, and C. Villareal, Europhys. Lett. **67**, 191 (2004).
[42] P. A. Maia Neto, A. Lambrecht, and S. Reynaud, Phys. Rev. A **78**, 012115 (2008).
[43] T. Emig, A. Hanke, R. Golestanian, and M. Kardar, Phys. Rev. Lett. **87**, 260402 (2001).
[44] A. Taleb, V. Russier, A. Courty, and M. P. Pileni, Phys. Rev. B **59**, 13350 (1999).
[45] N. Pinna, M. Maillard, A. Courty, V. Russier, and M. P. Pileni, Phys. Rev. B **66**, 045415 (2002).
[46] V. Yannopapas and N. Stefanou, Phys. Rev. B **69**, 012408 (2004).